Geophys. J. Int. (2006) **167,** 1309–1316 doi: 10.1111/j.1365-246X.2006.03093.x

Crustal constraints on the uplift mechanism of the Western Ghats of India

Pankaj Kr. Tiwari, G. Surve and G. Mohan

Department of Earth Sciences, Indian Institute of Technology Bombay, Powai, Mumbai—400076, *India. E-mail: gmohan@iitb.ac.in*

Accepted 2006 May 20. Received 2006 April 13; in original form 2005 November 1

SUMMARY

Over 800 receiver functions (RFs) from three broadband and five short period stations deployed in the northern segment of the Western Ghats of India, were analysed to examine the crustal constraints on the rift flank uplift mechanism of the Ghats. Estimates of Moho depths, mean shear velocities and Poisson's ratios were determined and used as constraints to model the RFs. The study reveals that the crust beneath the Ghats varies in thickness between 31 and 39 km and is neither uniformly thin nor thick as required by existing hypotheses for uplift mechanism. The Poisson's ratio is 0.26 and the mean shear velocity is 3.65 km s^{-1}. The uncertainties in the estimates of the Moho depths and Poisson's ratios are ± 2 km and ± 0.01, respectively. The crust beneath the Ghats is 3–4 km thinner than that beneath the adjoining low-lying coastal plains suggesting block tectonics. Modelling the RFs using crustal constraints reveals sub-Moho low-velocity zones (LVZs) with velocity reductions of 0.5–0.65 km s^{-1} which are confined to shallow depths of about 50 km beneath the Ghats. The persistent relief of the Ghats may be attributed to the buoyancy forces of the possibly rift related shallow upper mantle LVZs beneath the Ghats.

Key words: broadband, crustal structure, low-velocityzone, receiver function, Western Ghats.

INTRODUCTION

Passive continental margins represent the later mature stages of an active rift system formed due to extensional tectonics. Passive margins, the world over are characterized by the inland presence of linear, sea-facing escarpments which separate a lower elevation coastal plain from a low relief highland. Although scarp retreat is believed to be an established paradigm, Matmon *et al.* (2002) argue that the locations of the escarpments which are generally understood to have been developed due to rift flank uplift are exceptionally stable and determined by crustal structure. Marginal uplifts and the presence of elevated regions adjoining passive rifts are a common geological phenomena along nascent and juvenile continental margins, although the precise mechanism causing these uplifts remains debatable. The western margin of India forms one such passive continental margin which features the coast parallel great escarpment known as the Western Ghats or Sahyadris whose origin and nature of rift flank uplift have been the subject of morphological study debated over a century (Ollier 1985). Historically, the most commonly cited processes for the uplift are predominantly endogenic phenomena, which include rift related mechanisms of crustal thinning (McKenzie 1978), magmatic underplating (Cox 1980; Devey & Lightfoot 1986), transient thermal effects (Cochran 1983) and secondary convective effects associated with extension and flexural unloading (Buck 1986; Weissel & Karner 1989), denudational isostacy (Gilchrist & Summerfield 1994; Widdowson & Cox 1996; Gunnell 2001) and flexural response to denudation (Gunnell & Fleitout 2000). Gunnell (2001) provides a comprehensive review of the theoretical causes of plateau uplift which broadly fall into three categories with the underlying principles being isostatic response to reduction in density either caused mechanically or thermally (isostacy), increase in lithospheric thickness (crustal buoyancy), and, plastic necking due to lithospheric stretching or asymmetrical denudation on either side of the scarp (lithospheric flexure). Validation of any of these hypotheses is hampered by the relatively sparse geophysical mapping of the Ghats. The present study attempts to provide crustal seismological constraints on the mechanism of uplift of the Western Ghats through receiver function (RF) studies carried out in the northern volcanic segment of the Ghats in the Deccan Volcanic Province (DVP) of India (Fig. 1), complemented by other similar studies in the southern segment.

WESTERN GHATS

The Western Ghats of peninsular India extend in a NNW–SSE direction almost parallel to the west coast of India for over 1500 km with an average elevation of 1.2 km (Fig. 1). The Ghats begin from just south of Narmada rift and continue unbroken, with peaks as high as 8000 ft, up to Cape Comorin in the south, except for a break at Palghat. They form the dividing line between two erosional surfaces, the low-lying plains of marine denudational and a peneplaned

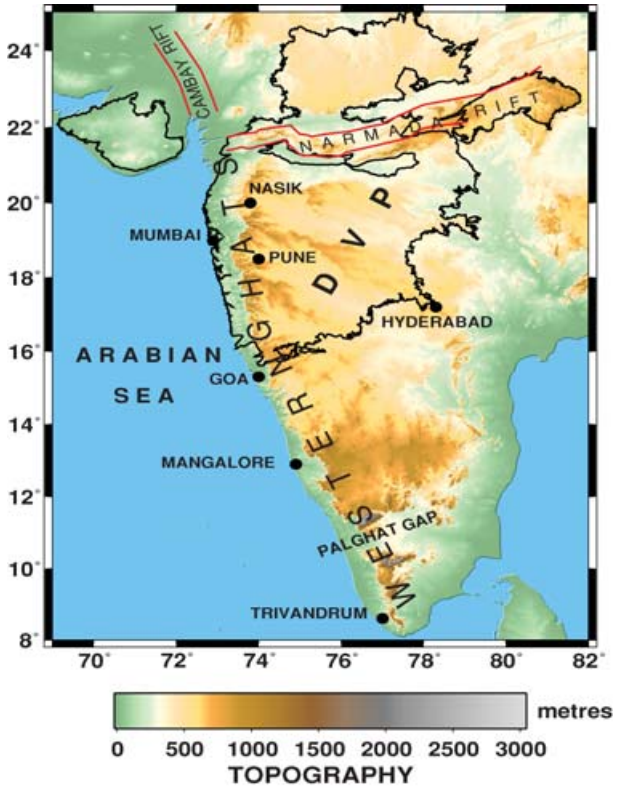

Figure 1. Tectonic map of western India overlain with the colour coded topography, showing the Western Ghats, the outline of the Deccan Volcanic Province(DVP) and other major tectonic features.

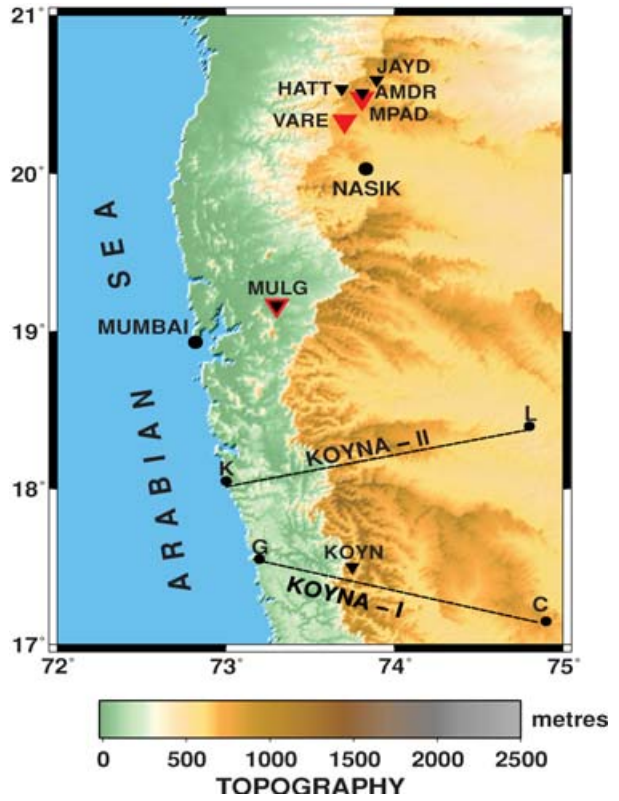

Figure 2. Map showing the location of seismic stations with the red and black symbols denoting broadband (CMG-3T) and short period (L-4C-3D) stations respectively. The Deep seismic sounding (DSS) profiles are denoted as Koyna I: G–C (Guhagar–Chorochi) and Koyna II: K–L (Kelsi–Loni).

plateau at elevations of over 1 km. The Ghats traverse many different geological formations of differing physical and structural characteristics. The northern half of the Ghats till Goa is formed of horizontal beds of massive Deccan trap. The region south of Goa till Palghat comprises of schists and gneisses and further south of Palghat are a complex group of hills made up of mainly charnockites.

DATA AND METHODOLOGY

Teleseismic waveform data in the epicentral distance range 30°–95° recorded by a temporary network of seismic stations comprising of three short period (L-4C-3D) (HATT, JAYD, AMDR) and two broadband (CMG-3T) stations (VARE, MPAD) deployed by the Indian Institute of Technology Bombay (IITB), in the northern half of the Western Ghats near Nasik (Fig. 2) during 2000–2003 were analysed. In addition, the short period as well as the broadband data from a coastal station (MULG) near Mumbai where a short period and a broadband station were deployed for three years each by IITB since 1998 was analysed. To extend the study further south, data from another short period station on the Ghats at Koyna (KOYN) operated by Maharashtra Engineering Research Institute (MERI) was also analysed (Fig. 2). The initially large data set was whittled down to over 800 traces with most stations JAYD(108), AMDR(156), HATT(121) and MULG (SP-103; BB-250) providing more than 100 traces each except for the stations MPAD(40), VARE(58) and KOYN(74) based on a signal to noise cut off ratio of 2.5. The average elevation of the stations on the Ghats is 800 m above mean sea level. The azimuthal distribution of the events used (Fig. 3) shows that most events are from the eastern azimuths with very few events recorded in the western azimuths.

The RF analysis involves isolation of the *P*-to-*S* converted phases from subsurface discontinuities through component rotation, while deconvolution eliminates the source effects from the waveforms (Langston 1979; Owens *et al.* 1984). In order to decompose the *P*, *SV* and *SH* wavefields, the *Z*, *N* and *E* components are rotated into *L*, *Q* and *T* ray coordinate system, where *L* is in the direction of the direct *P* phase, *Q* in the direction of the *SV* phase and *T* in the direction of the *SH* phase (Vinnik 1977; Kind 1985). Rotation within the vertical plane (i.e. from *Z*, *R* (radial) to *L*, *Q*) requires knowledge about the polarization angle of the *P* wave at the receiver, which is derived from the particle motion. Under the assumption of a laterally homogeneous structure, this angle is a function of the horizontal slowness of the wave and the near surface *S* velocity beneath the station (Ammon 1991). The *S* velocity is determined by measuring the amplitude at zero delay time of the direct *P* phase which is usually the dominant pulse in *R* component receiver functions (Ammon 1991). Once the waveforms are rotated into *L*, *Q*, *T*, the *L* component contains only the source pulse and the *Q* component contains the source pulse superposed on the scattered wavefield which encompasses both the converted phases (forward scattered) and multiples (backscattered). Deconvolving the *L* component from the *Q* component removes the source pulse leaving behind the Ps conversions and the multiples. A low-pass filter of 2 Hz was used to suppress the high-frequency noise. To compare the receiver functions at different slownesses and to distinguish converted phases from multiples, a moveout correction was applied separately for the converted phases and multiples. The correction was made for a reference slowness of 6.4 s/° corresponding to an epicentral distance of about 67° in the IASP91 model. Thus, for a horizontally stratified

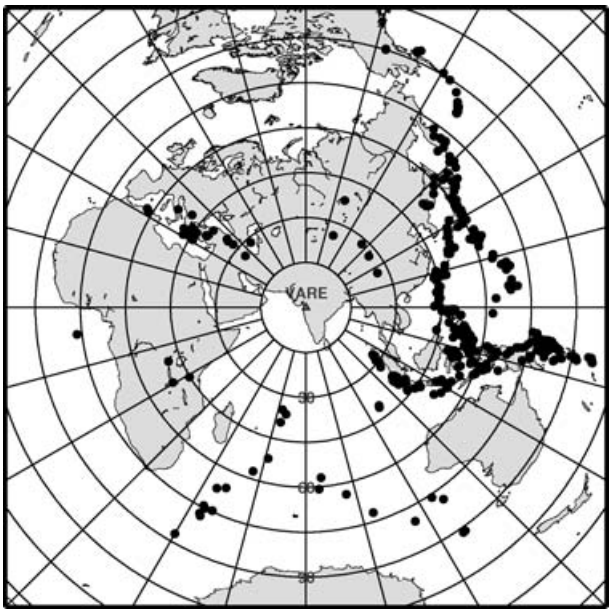

Figure 3. Azimuthal distribution of teleseismic events plotted with respect to station VARE.

media, the converted phases from interfaces at depth with different slownesses align parallel to the *P* phase while the multiples are inclined. To enhance the coherence of converted phases and multiples from an interface the receiver functions were stacked in narrow slowness bins.

RESULTS

The receiver functions (RFs) exhibit strong *P* to *S* conversions from the base of the Deccan traps and the Moho at all stations (Figs 4 and 5). The arrival times of the *Pms* conversions from the Moho range between 3.8 s at JAYD and 4.8 s at KOYN. The RFs computed from the broadband data at MULG and VARE show distinct Moho multiples *Ppms* and *Psms* which are used to determine the Poisson's ratio (σ) and crustal thickness (Z_M) following the approach of Zhu & Kanamori (2000). This technique involves a grid search over the σ and Z_M space to determine the (σ, Z_M) pair which best fits the observed *Pms*, *Ppms* and *Psms* waveforms. An average crustal *P*-velocity of 6.45 km s^{-1}, determined from the deep seismic sounding (DSS), along Koyna I and II profiles (Kaila *et al.* 1981a,b), was used to constrain the Moho depth. The average crustal thicknesses at MULG and VARE were estimated to be 36 and 35 km, respectively, while the Poisson's ratio was determined to be close to 0.26 $\pm$ 0.01 for both stations (Fig. 4). Similar results were obtained for the broadband station at MPAD. Using the Poisson's ratio (0.26) and the average crustal *P*-velocity (6.45 km s^{-1}) as constraints for the entire region, the average crustal thickness values at all the short period stations were determined to be varying between 31 and 39 km. Interestingly, both the short period stations (HATT, JAYD) within a close network in the northernmost part of the Ghats exhibit a 3–4 km thinner crust compared to that beneath the well spread out broadband stations on the Ghats (Fig. 2) at VARE, MPAD and MULG, which provide better estimates of the Moho depths due to constraints imposed by the presence of distinct Moho multiples. To ascertain the reliability of the results obtained from short period stations, the data from the short period station at MULG was analysed and the computed RFs (Fig. 5) compared with the Broadband RFs (Fig. 4)

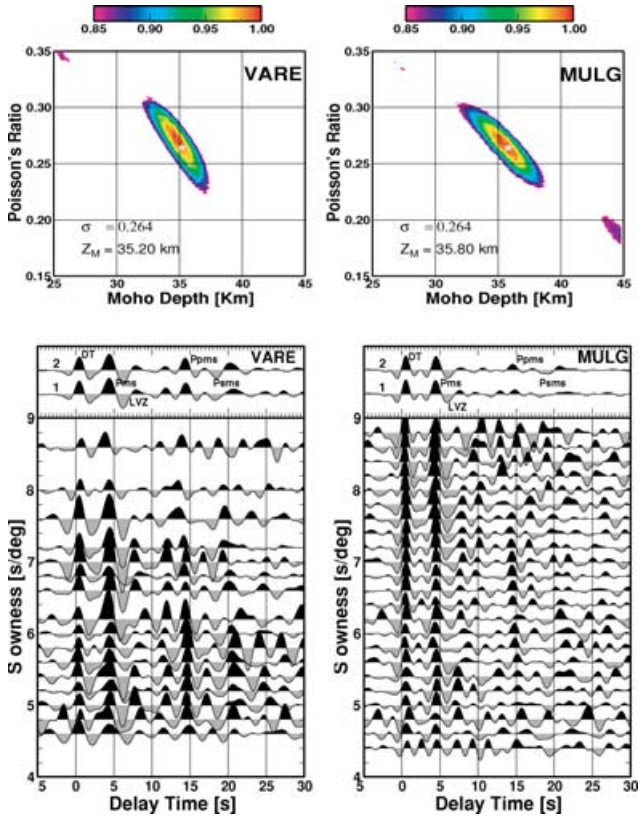

Figure 4. (Bottom) Plots of the *SV* receiver functions for VARE and MULG averaged over narrow slowness bins. The Moho *P*-to-*S* converted phase (*Pms*) and Moho multiples *Ppms* and *Psms* are indicated in the summation traces shown on top. DT denotes the converted phase from the base of the Deccan Traps and the negative phase following the *Pms* is denoted as LVZ. (Top) Determination of the average crustal Poisson's ratio for VARE and MULG. The colour scale indicates normalized contour values.

obtained from the broadband station operated earlier at the same site. It is observed that the arrival time of the *Pms* phase is the same for both short period and broadband stations and consequently, the depth to the Moho is similar in both cases. A similar exercise was carried out at VARE using both short period and broadband data and consistent results were obtained. Thus, the determination of the crustal thicknesses through the short period stations (JAYD, HATT, AMDR and KOYN) is found to be reliable.

UNCERTAINTIES IN CRUSTAL THICKNESSES

Uncertainties in the estimates of crustal thicknesses (Z_M) could arise from variations in the assumed average crustal *P*-wave velocities (*Vp*) and crustal Poisson's ratio (σ) as well as errors in time picks of *Pms* and multiples (*Ppms*). The average crustal *Vp* in India derived from DSS (Reddy *et al.* 1999) varies from 6.2 km s^{-1} in sedimentary basins to 6.6 km s^{-1} in the Cambay rift. In DVP, *Vp* averages 6.45 km s^{-1} along both the Koyna profiles which cut across the Western Ghats. To ascertain the uncertainties in the crustal thickness arising for a possible range of *P*-wave velocities, the values for *Vs*, σ and Z_M were determined for slowness (p) of 6.4 s/° using the expression given below (eq. 1) for a suit of *Vp* values in the range 6.45 $\pm$ 0.1 km s^{-1}, as per the approach of Zandt *et al.* (1995) and Last *et al.* (1997), and the results summarized in Table 1.

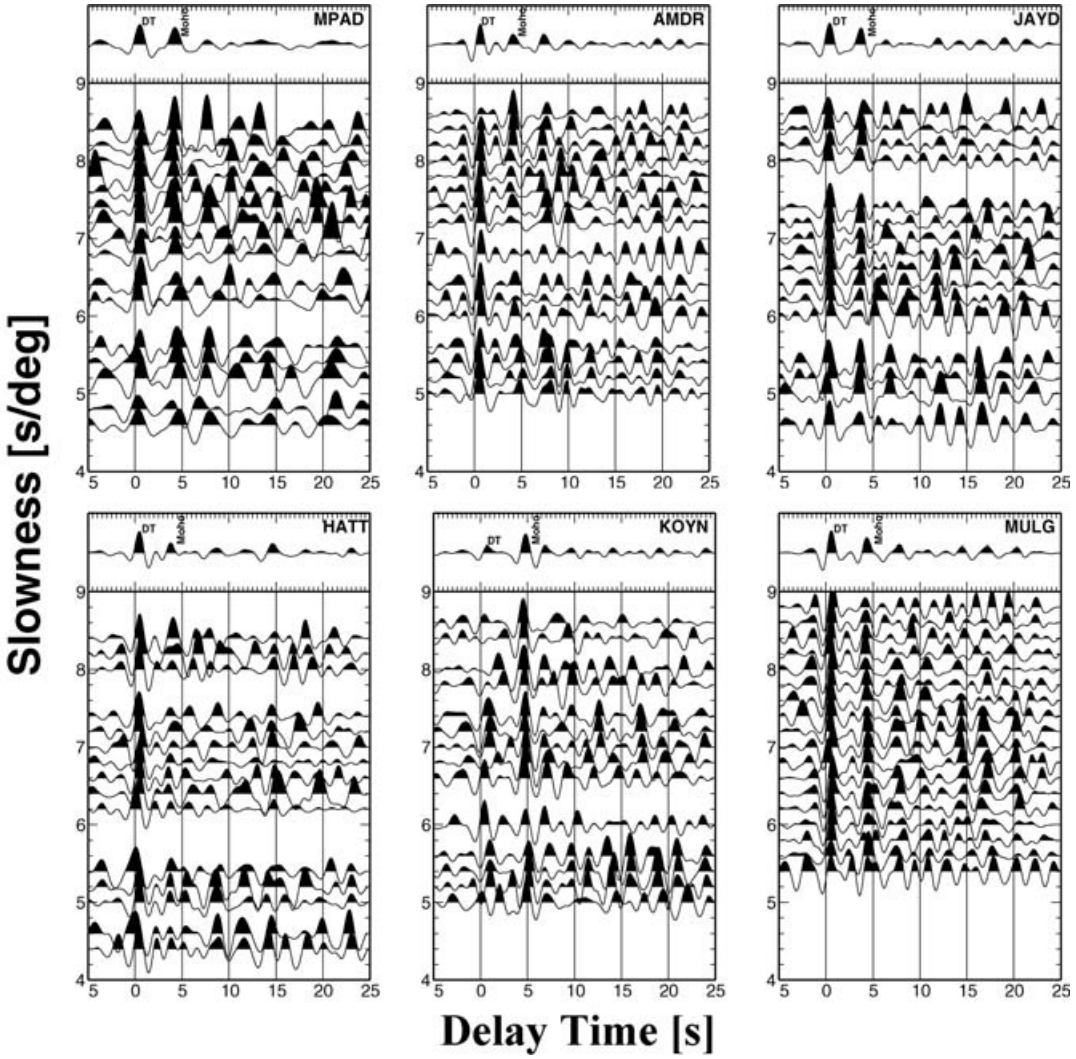

Figure 5. Receiver functions moveout corrected for the converted phases (*Pms*) and stacked in narrow slowness bins. The summation trace is shown on top. The labels DT and Moho denote the converted phases from the base of the Deccan traps and the Moho, respectively.

Table 1. Results of receiver function analysis for a range of plausible mean crustal *P*-wave velocities.

		$Vp = 6.35\,\mathrm{km\,s^{-1}}$		$Vp = 6.40\,\mathrm{km\,s^{-1}}$		$Vp = 6.45\,\mathrm{km\,s^{-1}}$		$Vp = 6.50\,\mathrm{km\,s^{-1}}$		$Vp = 6.55\,\mathrm{km\,s^{-1}}$	
Stations	Moho Phases Arrival Time (s) T_{Pms}, T_{Ppms}	*Vs* ($\mathrm{km\,s^{-1}}$)	Moho Depth (km)	*Vs* ($\mathrm{km\,s^{-1}}$)	Moho Depth (km)	*Vs* ($\mathrm{km\,s^{-1}}$)	Moho Depth (km)	*Vs* ($\mathrm{km\,s^{-1}}$)	Moho Depth (km)	*Vs* ($\mathrm{km\,s^{-1}}$)	Moho Depth (km)
VARE	4.35, 14.45	3.59	34.51	3.62	34.82	3.65	35.14	3.68	35.46	3.72	35.78
MPAD	4.20, 13.80	3.57	32.80	3.60	33.10	3.63	33.40	3.66	33.70	3.69	34.01
AMDR	4.15 —	3.62	33.47	3.64	33.71	3.67	33.95	3.70	34.19	3.73	34.43
JAYD	3.80 —	3.62	30.65	3.64	30.87	3.67	31.09	3.70	31.31	3.73	31.52
HATT	3.80 —	3.62	30.65	3.64	30.87	3.67	31.09	3.70	31.31	3.73	31.52
MULG	4.35, 14.55	3.61	34.85	3.64	35.17	3.67	35.49	3.70	35.81	3.73	36.13
KOYN	4.80 —	3.62	38.71	3.64	38.99	3.67	39.27	3.70	39.54	3.73	39.82

$$Vp/Vs = \left\{(1 - p^2Vp^2)\left[2\left(t_{Pms} - t_p\right)/(t_{Ppms} - t_{Pms}\right) + 1\right]^2 + p^2Vp^2\right\}^{1/2}. \quad (1)$$

It is observed that *Vs* varies between 3.57 and 3.73 km s^{-1}, averaging 3.65 km s^{-1} and the crustal thickness varies between 31 and 39 km while the Poisson's ratio is similar for the three broadband stations VARE, MULG and MPAD. The errors in timings of *Pms* and *Ppms* of ±0.05 s translate to errors of <0.5 km in Z_M. The uncertainties in the average crustal thickness for *P* velocity of 6.45 ± 0.10 km s^{-1} and Poisson's ratio of 0.26 ± 0.01 are ±0.5 km and ±1 km, respectively (Table 2), which together translate to an uncertainty of about ±2 km in the crustal thickness.

SYNTHETICS

The RFs at VARE, MPAD and MULG exhibit a prominent negative phase immediately following the *Pms* phase (Figs 4 and 5).

Table 2. Uncertainties in the estimates of crustal thicknesses for a range of *P*-wave velocities and Poisson's ratios.

	$Vp = 6.35\,\mathrm{km\,s^{-1}}$		$Vp = 6.40\,\mathrm{km\,s^{-1}}$		$Vp = 6.45\,\mathrm{km\,s^{-1}}$		$Vp = 6.50\,\mathrm{km\,s^{-1}}$		$Vp = 6.55\,\mathrm{km\,s^{-1}}$	
Poisson's Ratio	*Vs* ($\mathrm{km\,s^{-1}}$)	Moho Depth (km)	*Vs* ($\mathrm{km\,s^{-1}}$)	Moho Depth (km)	*Vs* ($\mathrm{km\,s^{-1}}$)	Moho Depth (km)	*Vs* ($\mathrm{km\,s^{-1}}$)	Moho Depth (km)	*Vs* ($\mathrm{km\,s^{-1}}$)	Moho Depth (km)
0.250	3.67	36.21	3.70	36.47	3.72	36.72	3.75	36.98	3.78	37.24
0.255	3.64	35.64	3.67	35.90	3.70	36.16	3.73	36.41	3.76	36.66
0.260	3.62	35.08	3.64	35.33	3.67	35.59	3.70	35.84	3.73	36.09
0.265	3.59	34.52	3.62	34.77	3.65	35.01	3.68	35.26	3.70	35.51
0.270	3.56	33.95	3.59	34.20	3.62	34.44	3.65	34.68	3.68	34.93

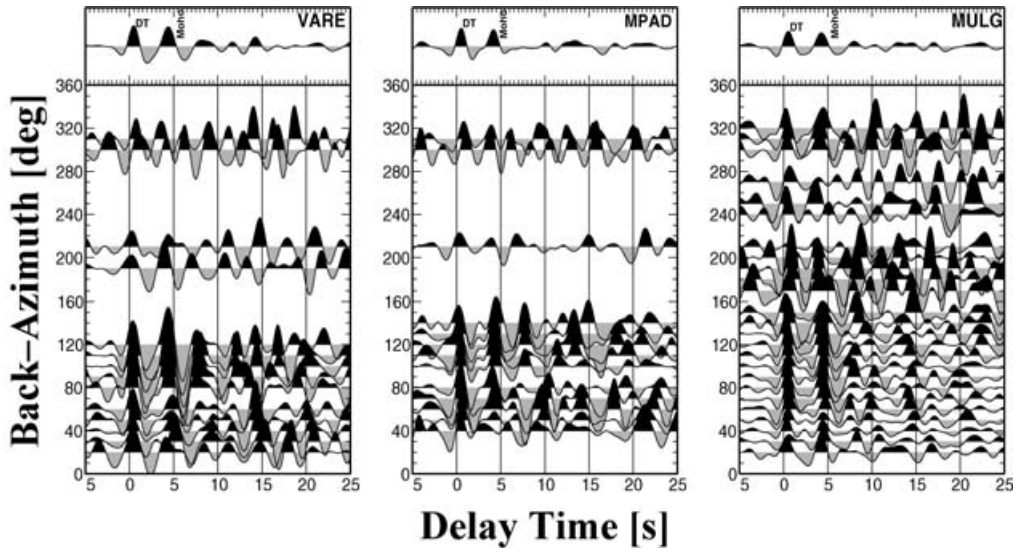

Figure 6. Backazimuth RF plots for VARE, MPAD and MULG moveout corrected for the converted phases and stacked in narrow back azimuth bins.

Such negative phases which could correspond to sub-Moho low-velocity zones (LVZ) are also clearly observed in most azimuths of the backazimuth RF plots at these stations (Fig. 6), which indicate a dependence of the arrival times of the negative phase on azimuth, suggesting variable depth of the causative. A negative phase is also consistently observed before the *Pms*, which may be a multiple from an intracrustal layer but cannot be confirmed due to lack of primary conversions from that layer. Synthetic RFs were generated using the reflectivity method (Mueller 1985) to model the observed *Pms*, the negative phase following the *Pms*, and the Moho multiples in the stacked waveform at the broadband stations VARE, MPAD and MULG (Fig. 7). A 35-km-thick crust with an average shear velocity of 3.65 $\mathrm{km\,s^{-1}}$ together with a velocity contrast of 0.55 $\mathrm{km\,s^{-1}}$ across a 4 km thick gradational Moho followed by a velocity reduction of 0.65 $\mathrm{km\,s^{-1}}$ from a depth of 50 km explains the observed waveforms at VARE. A similar negative phase with lower magnitude is observed at both MPAD and MULG stations which is explained by lowering of velocities with a gradient of 0.4 $\mathrm{km\,s^{-1}}$ (Fig. 7). The waveform modelling consistently exhibits the presence of an LVZ at sub-Moho depths of about 50 km without invoking any crustal layering. The arguments in favour of a sub-Moho LVZ are strengthened by the presence of negative isostatic anomalies ranging between −40 and −70 MGals (NGRI 1975) all along the Ghats (Fig. 8), which can be explained in terms of a thick crust or a sub-Moho LVZ. In the absence of an anomalously thick crust, the presence of a sub-Moho LVZ is the most likely explanation for the observed isostatic anomaly.

DISCUSSION

The results obtained in the present study together with published results are summarized in Fig. 8 which depicts the topography map of India on which the Airy isostatic gravity anomaly (NGRI 1975) contours corresponding to the −30, −50 and −70 MGals contour values are superimposed. The present study indicates that the crustal thickness beneath the Western Ghats varies from 31 to 39 km. Earlier, a crustal thickness of 36 km was reported beneath other stations, namely, PUNE and KARD on the Ghats through RF studies (Kumar *et al.* 2001). The east–west-trending DSS profile Koyna–I at Koyna, across the Ghats also indicates a crustal thickness of 37 km in the eastern block (east of Koyna) and about 40 km in the western block (Kaila *et al.* 1981a). Considering the crustal estimates from the present and earlier studies, the average crustal thickness beneath the Ghats is observed to be 36 km. However, the crustal thickness varies between 38 and 41 km in the Konkan coastal plains near Mumbai (Mohan & Kumar 2004) while it is 40 km at GOA (at the periphery of the DVP) and Mangalore (MNGR) (Sarkar *et al.* 2003), which are about 300 and 700 km south of Mumbai, respectively (Fig. 8). The crustal configuration of the Ghats and the coastal plains provide important constraints on the uplift mechanism of the Ghats. Among the various mechanisms proposed for the uplift of the Western Ghats, at least two of them are directly dependent on the crustal structure. First, the crustal buoyancy model, which requires an additional mass at the surface or at the base of the crust in terms of underplating. Second, the isostatic model which seeks a

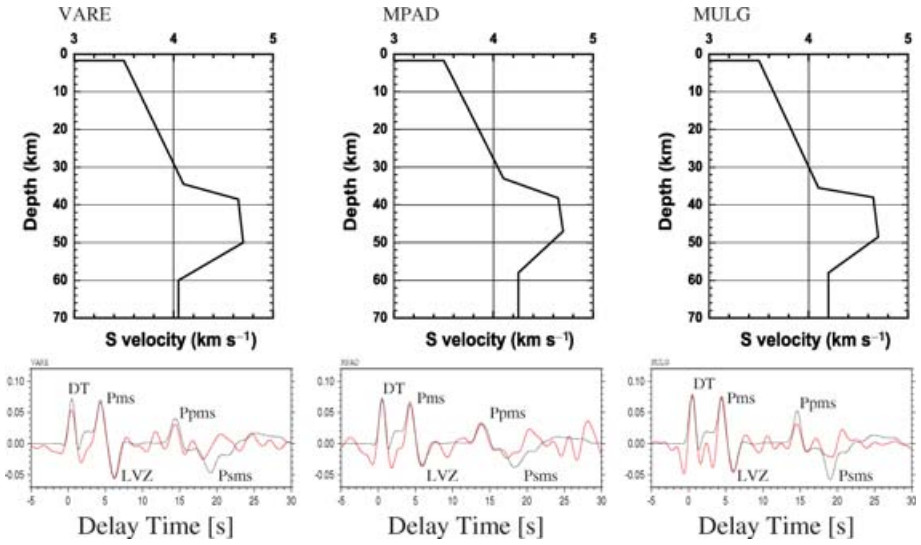

Figure 7. Comparison of observed stack (solid line) and synthetic (dotted line) *SV* receiver functions for VARE, MPAD and MULG corresponding to the respective shear wave velocity models (Top).

reduction in density caused either mechanically due to reduction in mass by erosion or thermally by the effects of a local heat source. The present study indicates that the crust is neither uniformly thin nor thick as required to justify the proposed models for the uplift mechanism. The observed variations in the crustal thicknesses may be a result of block tectonics as evidenced from the DSS profiles at Koyna across the Ghats. The Poisson's ratio at VARE is 0.26, which is similar to that observed at other stations along the Ghats at MULG (Mohan & Kumar 2004) and PUNE and KARD (Kumar *et al.* 2001). The average crustal thickness of 36 km beneath the Ghats together with the low Poisson's ratio, therefore, do not support the possibility of magmatic underplating as a feasible model for explaining the uplift. Chand & Subrahmanyam (2003) conclude through admittance analysis of gravity data on the western margin of India, that at least 8 km of underplating would be required to fit the observed gravity anomaly and rule out the underplating model, since the topography of the Ghats increases towards south away from the northern volcanic segment of the Ghats. In the absence of any conclusive evidences supporting the existing theories based on the crustal thicknesses beneath the Ghats, the persistence elevation over time needs to be examined in the light of the surrounding structure as well as the sub-Moho structure.

The coastal stations near Mumbai in the northern volcanic half of the Ghats up to MNGR in the southern portion are underlain by a thick crust averaging 40 km (Sarkar *et al.* 2003; Mohan & Kumar 2004), which is significantly thicker than that beneath the adjoining Ghats (Fig. 8). The pronounced difference in the crustal thicknesses at the coast and away from it beneath the Ghats gives rise to the possibility of block faulting and reflects the role of vertical tectonics in the uplift mechanism of the Ghats. Presence of north–south-trending structural features like the horst-graben structures off the west coast in the Arabian sea in support of a series of normal faulting are reported by Biswas (1987). Geomorphological evidences also support the theory that the Ghats are a consequence of Cenozoic uplift, rifting and down faulting (Radhakrishna 1993). Still, the persistent elevation of the Ghats over time is a puzzling phenomena which is not satisfactorily resolved. The consistently negative isostatic anomalies (-40 to -70 MGals) that appear seaward of the Western Ghats escarpment (Fig. 8) are interpreted to be due to magmatic underplating, a thickened crust, lithospheric/crustal thinning or a low-density upper mantle (Gunnell 2001). The present study does not support the first three options leaving the low-density upper mantle to be the only option to be examined. 2-D modelling of the gravity data available on land and ocean (Pandey *et al.* 1996) reveals an extensive sub-Moho low-density (2.95–3.05 g cm^{-3}) zone extending beneath the western continental margin of India near Mumbai at depths of 45–60 km. This low-density upper mantle correlates well with the low-velocity zone delineated at shallow depths of about 50 km beneath the Ghats in the present study. Earlier, a low-velocity zone was identified at a depth of 56 km beneath the Koyna profile through waveform modelling (Krishna 1991). Although the southward extension of the LVZ beyond KARD is not mapped, the RFs at GOA and MNGR exhibit a negative phase following the *Pms* arrival, probably corresponding to an LVZ, which however is not modelled (Sarkar *et al.* 2003). While the low-density layer reported (Pandey *et al.* 1996) is based on widely spaced gravity data and is modelled to be uniform, the LVZ delineated in the present study is non-uniform and varies in magnitude between stations. The upper mantle image down to 700 km beneath DVP reveals that the LVZ is confined only to the shallow upper mantle and, therefore, maybe unrelated to any large scale processes such as the Deccan episode (Ravi Kumar & Mohan 2005). Low-velocity zones are manifestations of thermal/chemical anomalies associated with regional/local causatives. Although partial melting due to thermal anomalies is a preferred explanation for the sub-Moho LVZ observed beneath young volcanic regions like Arabia (Kumar *et al.* 2002) and Basin and Range provinces (Benz & McCarthy 1994) there are several other causes which could result in LVZs. Presence of even small amounts of melts or fluids ($<$1–2 per cent) can decrease the seismic velocity substantially (Mavko 1980). Experiments have shown that presence of carbonate reduces the solidus temperature resulting in melting and development of LVZ (Presnall & Gudfinnson 2005). It is possible that the origin of the LVZ may not be linked to the evolution of the DVP but may be related to the rifting of the Indian plate since it appears to be confined to the continental margin. The western continental margin of India is a passive margin which rifted from Madagascar and later Seychelles about 85 and 65 Ma ago, respectively. The tomograms in the north western part of DVP and

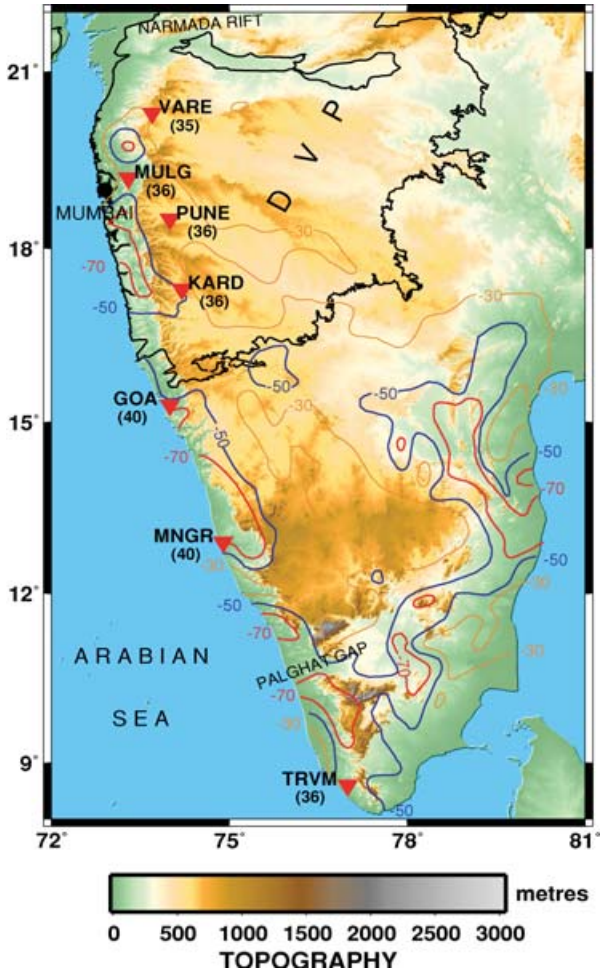

Figure 8. Map depicting the Moho depths (km) determined from the present study and earlier studies plotted on a colour coded topographic map. The coloured contour lines represent the isostatic gravity anomaly (NGRI 1975) values corresponding to −30, −50 and −70 MGals. The crustal thicknesses (km) for (PUNE, KARD, TRVM) and (GOA, MNGR) are taken from Kumar *et al.* (2001) and Sarkar *et al.* (2003), respectively.

the adjoining Arabian sea do indicate low-velocity zones (Ramesh *et al.* 1993) possibly related to rifting. Thus, a distinct possibility is that the west coast rift flank may possibly preserve rift related relicts extending non-uniformly into the continental segment which are observed as LVZs. It is quite likely that the buoyancy forces of the shallow upper mantle LVZ extending laterally beneath the Ghats for over 400 km and possibly extending up to MNGR and beyond, explain the persistent relief of the Western Ghats. These conclusions would also be consistent with the negative isostatic anomalies observed over the Ghats.

ACKNOWLEDGMENTS

The authors thank Dr M. Ravi Kumar for his critical review. The financial support provided by the State Government of Maharashtra is acknowledged. The single station data from MERI is gratefully acknowledged.

REFERENCES

Ammon, C.J., 1991. The isolation of receiver effects from teleseismic *P* waveforms, *Bull. seism. Soc. Am.,* **81,** 2504–2510.

Benz, H.M. & McCarthy, I., 1994. Evidence for an upper mantle low velocity zone beneath the southern Basin and Range-Colarado plateau transition zone, *Geophys. Res. Lett.,* **21,** 509–512.

Biswas, S.K., 1987. Regional tectonic framework, structure and evolution of the western marginal basins of India, *Tectonophysics,* **135,** 307–327.

Buck, W.R., 1986. Small scale convection induced by passing rifting: the cause of uplift of rift shoulders, *Earth planet. Sci. Lett.,* **77,** 362–372.

Cochran, J.R., 1983. Effects of finite extension times on the development of sedimentary basins, *Earth planet. Sci. Lett.,* **66,** 289–302.

Chand, S. & Subrahmanyam, C., 2003. Rifting between India and Madagascar- mechanism and isostacy, *Earth planet. Sci. Lett.,* **210,** 317–332.

Cox, K.G., 1980, A model for flood basalt volcanism, *J. Petrol.,* **21,** 629–650.

Devey, C.W. & Lightfoot, P.C., 1986. Volcanological and tectonic control of stratigraphy and structure in the western Deccan traps, *Bull. Volcanol.,* **48,** 195–207.

Gilchrist, A.R. & Summerfield, M.A., 1994. Tectonics model of passive margin evolution and their implications for theories of long term landscape development, in *Process Models and Theoretical Geomorphology,* pp. 55–84, ed. Kirby, M.J., John Wiley and Sons Ltd.

Gunnell, Y., 2001. Dynamics and kinematics of rifting and uplift at the western continental margin of India, Insights from geophysics and numerical models, in *Sahyadri, the Great Escarpment of the Indian Subcontinent,* pp. 475–496, eds, Gunnell, Y. &Radhakrishna, B.P., Geological Society of India, Memoir No. 47, Bangalore, India.

Gunnell, Y. & Fleitout, L., 2000. Morphotectonic evolution of the Western Ghats, India, in *Geomorphology and Global Tectonics,* pp. 321–338, ed. Summerfield, M., John Wiley and Sons.

Kaila, K.L., Reddy, P.R., Dixit, M.M. & Lazarenko, M.A., 1981a. Deep crustal structure at Koyna, Maharashtra, indicated by deep seismic soundings, *J. Geol. Soc. of India,* **22,** 1–16.

Kaila, K.L., Murthy, P.R.K., Rao, V.K. & Kharetchko, G.E., 1981b. Crustal structure from deep seismic soundings along the Koyna II (Kelsi-Loni) profile, in the Deccan trap area, India, *Tectonophysics,* **73,** 365–384.

Kind, R., 1985. The reflectivity method for different source and receiver structures and comparison with GRF data, *J. Geophys.,* **58,** 146–152.

Krishna, V.G., 1991. Low velocity layers in the sub-crustal lithosphere beneath the Deccan Trap region of western India, *Phys. Earth planet. Int.,* **67,** 288–302.

Kumar, M.R., Saul, J., Sarkar, D., Kind, R. & Shukla, A.K., 2001. Crustal structure of the Indian shield: new constraints from teleseismic receiver functions, *Geophys. Res. Lett.,* **28,** 1339–1342.

Kumar, M.R., Ramesh, D.S., Saul, J., Sarkar, D. & Kind, R., 2002. Crustal structure and upper mantle stratigraphy of the Arabian shield, *Geophys. Res. Lett.,* **29**(8), doi:10.1029/2001GL014530.

Langston, C.A., 1979. Structure under Mount Rainer, Washington, inferred from teleseismic body waves, *J. geophys. Res.,* **84,** 4749–4762.

Last, R.J., Nyblade, A.A., Langston, C.A. & Owens, T.J., 1997. Crustal structure of the East African Plateau from receiver functions and Rayleigh wave phase velocities, *J. geophy. Res.,* **102**(B11), 24 469–24 483.

Matmon, A., Blerman, P. & Enzel, Y., 2002. Pattern and tempo of great escarpment erosion, *Geol. Soc. Am.,* **30**(12), 1135–1138.

Mavko, G.M., 1980. Velocity and attenuation in partially melted rocks, *J. geophys. Res.,* **85**(1980) 5173–5189.

McKenzie, D., 1978. Some remarks on the development of sedimentary basins, *Earth planet. Sci. Lett.,* **40,** 25–32.

Mohan, G. & Kumar, M.R., 2004. Seismological constraints on the structure and composition of western Deccan volcanic province from converted phases, *Geophys. Res. Lett.,* **31,** L02601, doi:10.1029/2003GL018920.

Mueller, G., 1985. The reflectivity method: a tutorial, *J. Geophys.,* **58,** 153–174.

NGRI, 1975. Gravity maps of India, National Geophysical Research Institute, Hyderabad, India.

Ollier, C.D., 1985. Morphotectonics of continental margins with great escarpments, in *Tectonic Geomorphology,* pp. 2–25, eds, Morosawa, M. & Hack, J.T., Allen and Unwin, Boston and London.

Owens, T.J., Zandt, G. & Taylor, S.R., 1984. Seismic evidence for an ancient rift beneath the Cumberland plateau, Tennessee, *J. geophys. Res.,* **116,** 618–636.

Pandey, O.P., Agarwal, P.K. & Negi, J.G., 1996. Evidence of low density sub-crustal underplating beneath western continental region of India and adjacent Arabian sea: geodynamical considerations, *J. Geodyn.,* **21,** 365–377.

Presnall, D.C. & Gudfinnson, G.H., 2005. Carbonate rich melts in the oceanic low velocity zone and deep mantle, in *Plates, plumes and paradigms,* pp. 207–216, eds Foulger, G.R., Natland, J.H., Presnall, D.C. & Anderson, D.L., Geol. Soc. Am. Special paper, 388.

Radhakrishna, B.P., 1993. Neogene uplift and geomorphic rejuvenation of the Indian peninsula, *Current Science,* **64,** 787–793.

Ramesh, D.S., Srinagesh, D., Rai, S.S., Prakasam, K.S. & Gaur, V.K., 1993, High-velocity anomaly under the Deccan Volcanic Province, *Phys. Earth planet. Sci.,* **77,** 285–296.

Ravi Kumar, M. & Mohan G., 2005. Mantle discontinuities beneath the Deccan volcanic province, *Earth planet Sci. Lett.,* **237,** 252–263.

Reddy, P.R., Venkateswarlu, N., Koteswara Rao, P. & Prasad, A.S.S.S.R.S., 1999. Crustal structure of Peninsular Shield, India from DSS studies, *Current Science,* **77**(12), 606–611.

Sarkar, D., Ravi Kumar, M., Saul, J., Kind, R., Raju, P.S., Chadha, R.K. & Shukla, A.K., 2003. A receiver function perspective of the Dharwar craton (India) crustal structure, *Geophys. J. Int.,* **154,** 205–211.

Weissel, J.K. & Karner, G.D., 1989. Flexural uplift of rift flanks due to mechanical unloading of the lithosphere during extension, *J. geophys. Res.,* **94,** 13 919–13 950.

Widdowson, M. & Cox, K.G., 1996. Uplift and erosional history of the Deccan traps, India: evidence from laterites and drainage patterns of the western ghats and konkan coast, *Earth planet. Sci. Lett.,* **137,** 57–69.

Vinnik, L.P., 1977. Detection of waves converted from *P* to *SV* in the mantle, *Phys. Earth planet. Inter.,* **15,** 39–45.

Zandt, G., Myers, S.C. & Wallace, T.C., 1995. Crust and mantle structure across the Basin and Range-Colorado plateau boundary at 37°N latitude and implications for Cenozoic extension mechanism, *J. geophys. Res.,* **100,** 10 529–10 548.

Zhu, L. & Kanamori, H., 2000. Moho depth variation in southern California from teleseismic receiver functions, *J. geophys. Res.,* **105,** 2969–2980.